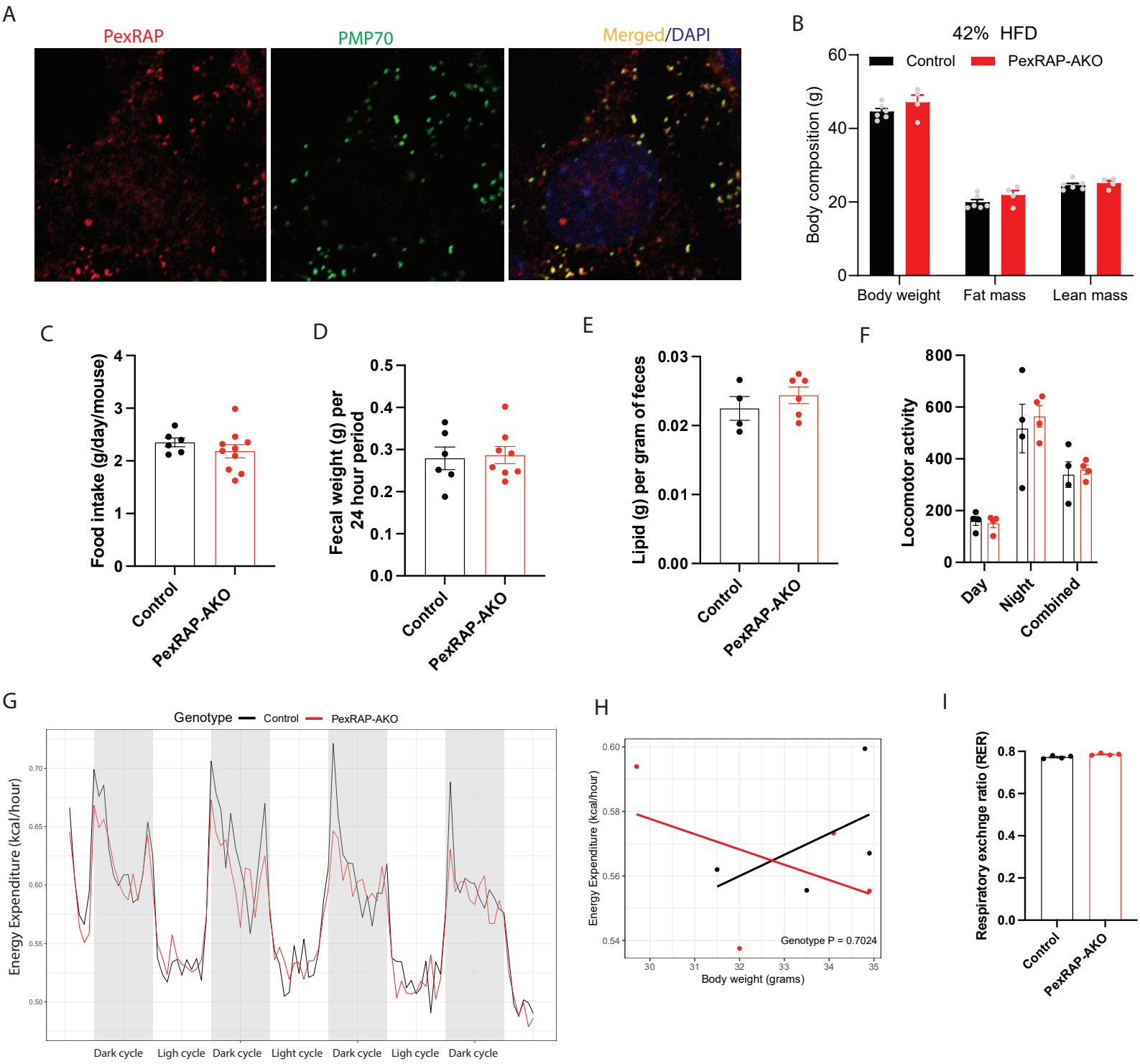

Supplementary Figure 1. Analysis of energy balance in PexRAP-AKO mice. **A**) Fluorescence microscopy of PexRAP (red), PMP70 (green) and DAPI (blue) in differentiated iWAT stromal vascular fraction cells. **B**) Body composition results from EchoMRI analysis of male control and PexRAP-AKO mice fed a HFD (42% kcal fat) for 16 weeks (n = 4-6). **C**) HFD (60% kcal fat) food intake (n = 6-10) **D**) daily fecal weight (n = 6-8) and **E**) normalized fecal fat content of control or PexRAP-AKO mice fed a HFD (60% kcal fat) for between 6-16 weeks (n = 4-6). Indirect calorimetry measurements of **F**) locomotor activity, **G- H**) energy expenditure, and **I**) respiratory exchange ratio (RER) from male control and PexRAP-AKO mice fed HFD (60% kcal fat) for 12 weeks (n = 4); lines of best fit represent results of an ANCOVA analysis. Data are shown as mean ± SE M. Comparisons between groups were made with a two-tailed unpaired Student's t-test (C,D,E,F, I) or an ANCOVA analysis to determine the effect of genotype on EE independent of body weight (H).

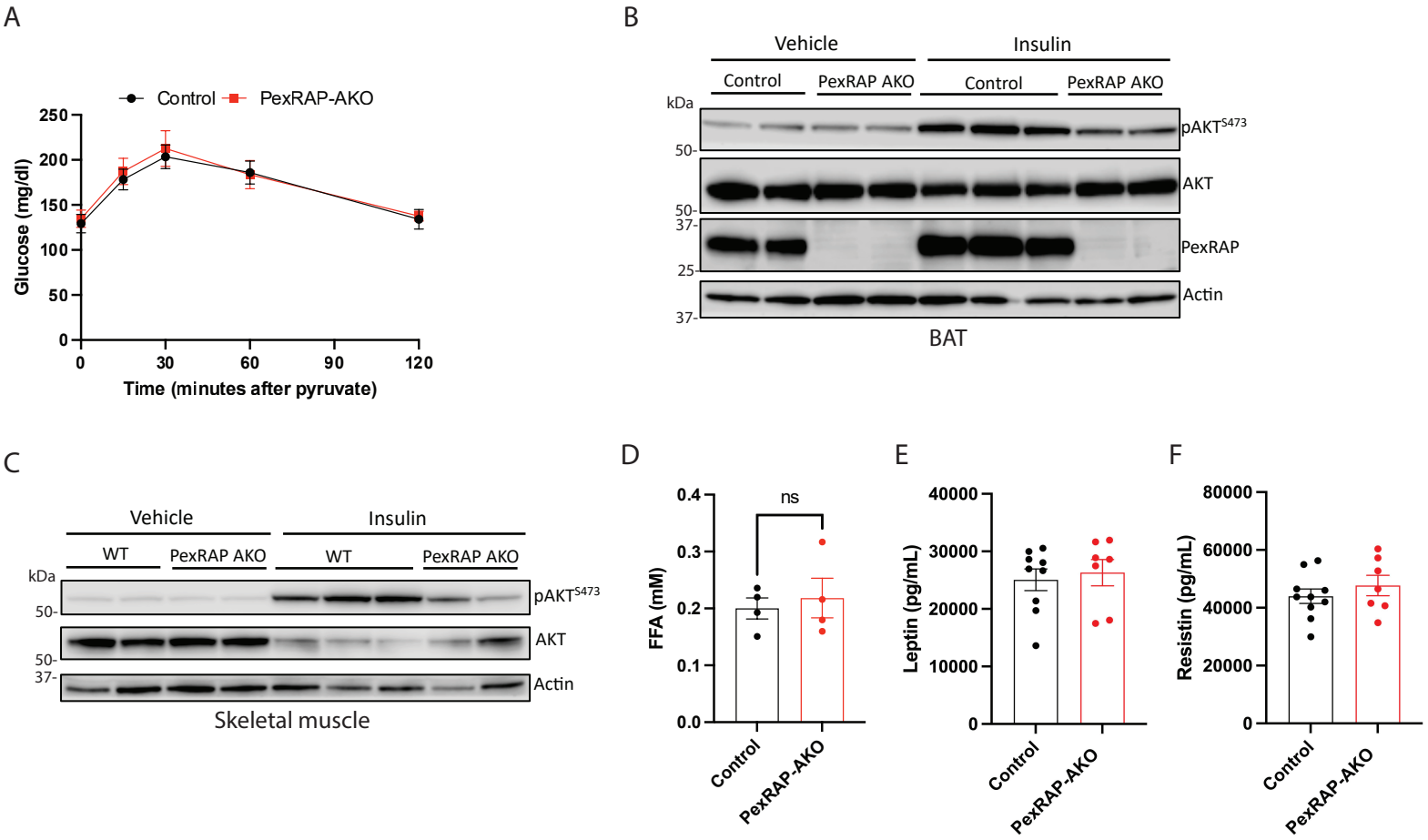

Supplementary Figure 2. Metabolic phenotyping in PexRAP-AKO mice. A) Pyruvate tolerance test of control or PexRAP-AKO mice fed a HFD (60% kcal fat) for 14 weeks (n = 7-9). **B-C**) Western blot analysis in BAT (**B**) and skeletal muscle (**C**) of male HFD-fed control or PexRAP-AKO mice injected intraperitoneally with vehicle or insulin. Tissues were harvested 10 minutes after insulin injection. AKT phosphorylation was analyzed at Ser473. **D**) Serum free fatty acid (FFA) levels of ad-libitum fed male control or PexRAP-AKO mice following 12 weeks of HFD feeding (n = 4). **E-F**) Serum levels of leptin and resistin from HFD fed male control and PexRAP-AKO mice (n = 7-9). Data are shown as mean ± SEM. Comparisons between groups were made with a two-tailed unpaired Student's t-test (A,D-F).

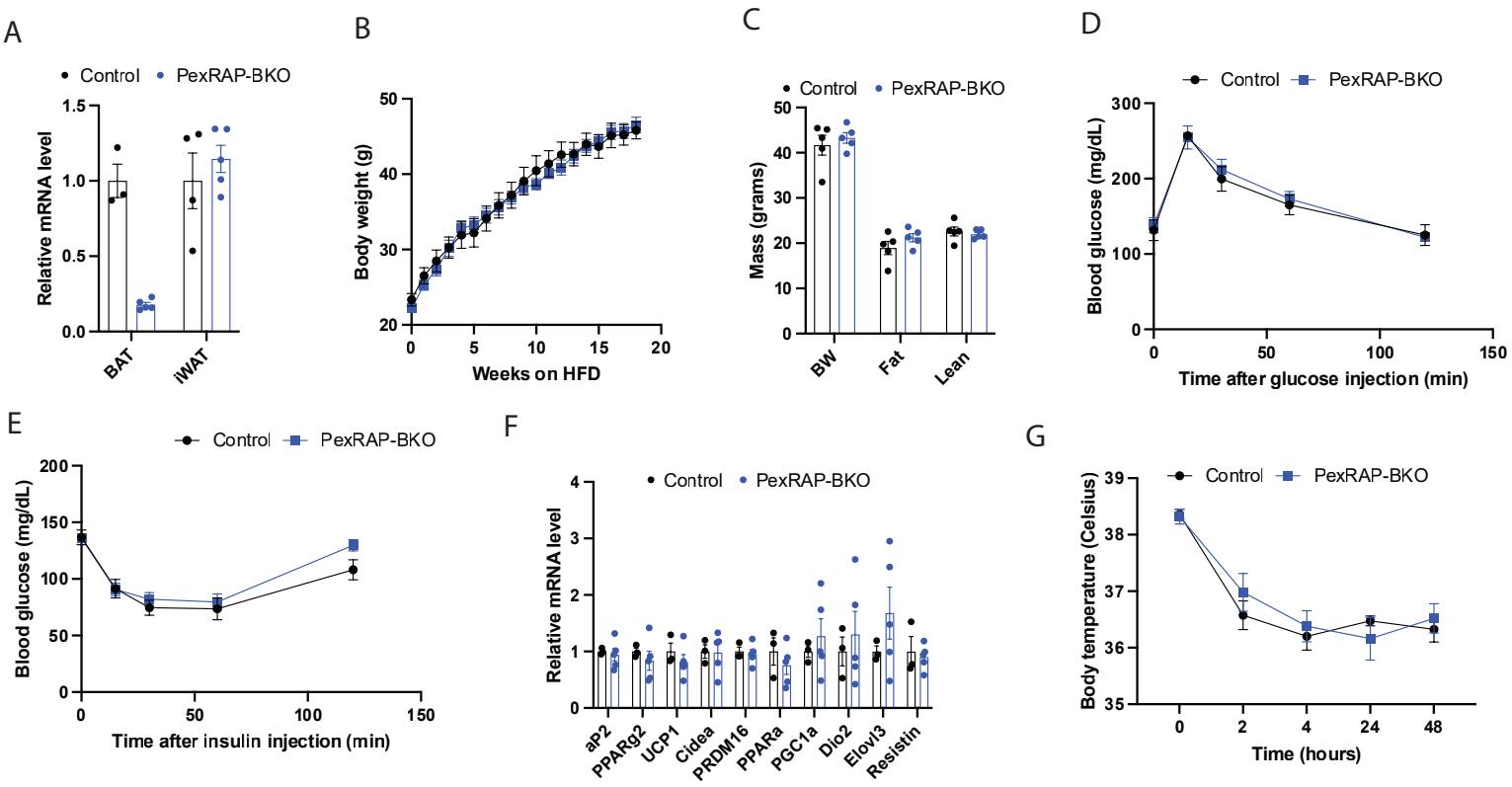

Supplementary Figure 3. BAT-specific knockout of PexRAP is not sufficient to affect adiposity or metabolism in HFD-fed mice. **A**) qPCR analysis of PexRAP mRNA levels in BAT and iWAT of UCP1-cre driven brown adipose tissue specific knockout mice (PexRAP-BKO) (n = 3-5). **B**) Body weights of control or male PexRAP-BKO mice fed a HFD (60% kcal fat) beginning at 6 weeks of age (n = 4-5). **C**) Echo-MRI analysis of body composition of control or PexRAP-BKO mice fed a HFD for 16 weeks (n = 5). **D**) Glucose tolerance test measurements in HFD-fed control and PexRAP-BKO mice (n = 5). **E**) Insulin tolerance test measurements of HFD-fed control or PexRAP-BKO mice (n = 9-12). **F**) qPCR analysis of thermogenic gene mRNA levels in BAT of chow-fed PexRAP-BKO mice (n = 3-5). **G**) Core body temperatures of male control and PexRAP-BKO mice upon exposure to 4°C ambient temperature (n = 4-5). Data are shown as mean ± SEM. Comparisons between groups were made with a two-tailed unpaired Student's t-test.

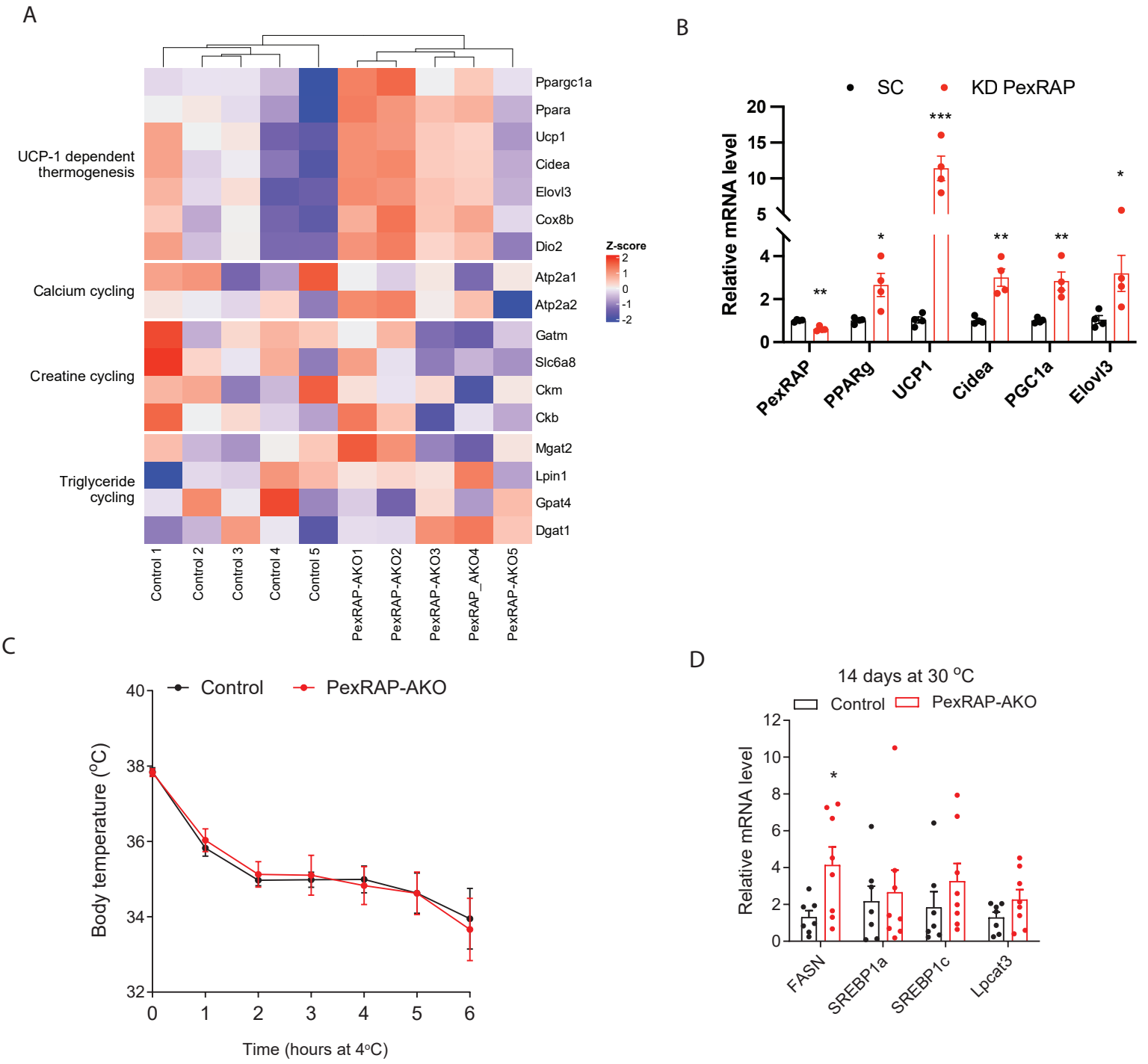

Supplementary Figure 4. Genes involved in UCP1-dependent thermogenesis are elevated in iWAT of PexRAP-AKO mice. **A**) Normalized expression of genes involved in UCP1-dependent and -independent thermogenesis in PexRAP-AKO RNA-seq dataset (n = 5). **B**) qPCR analysis of thermogenic gene expression in differentiated iWAT stromal vascular fraction cells after shRNA-mediated knockdown of PexRAP (n = 4). **C**) Body temperature of control (N=8) and PexRAP-AKO (N=7) mice after cold exposure. **D**) qPCR analysis of lipogenic gene expression in iWAT of control (N=7) and PexRAP-AKO (N=8) mice that were housed at thermoneutrality (30°C) for 14 days. Data are shown as mean ± SEM. Comparisons between groups were made with a two-tailed unpaired Student's t-test (B).

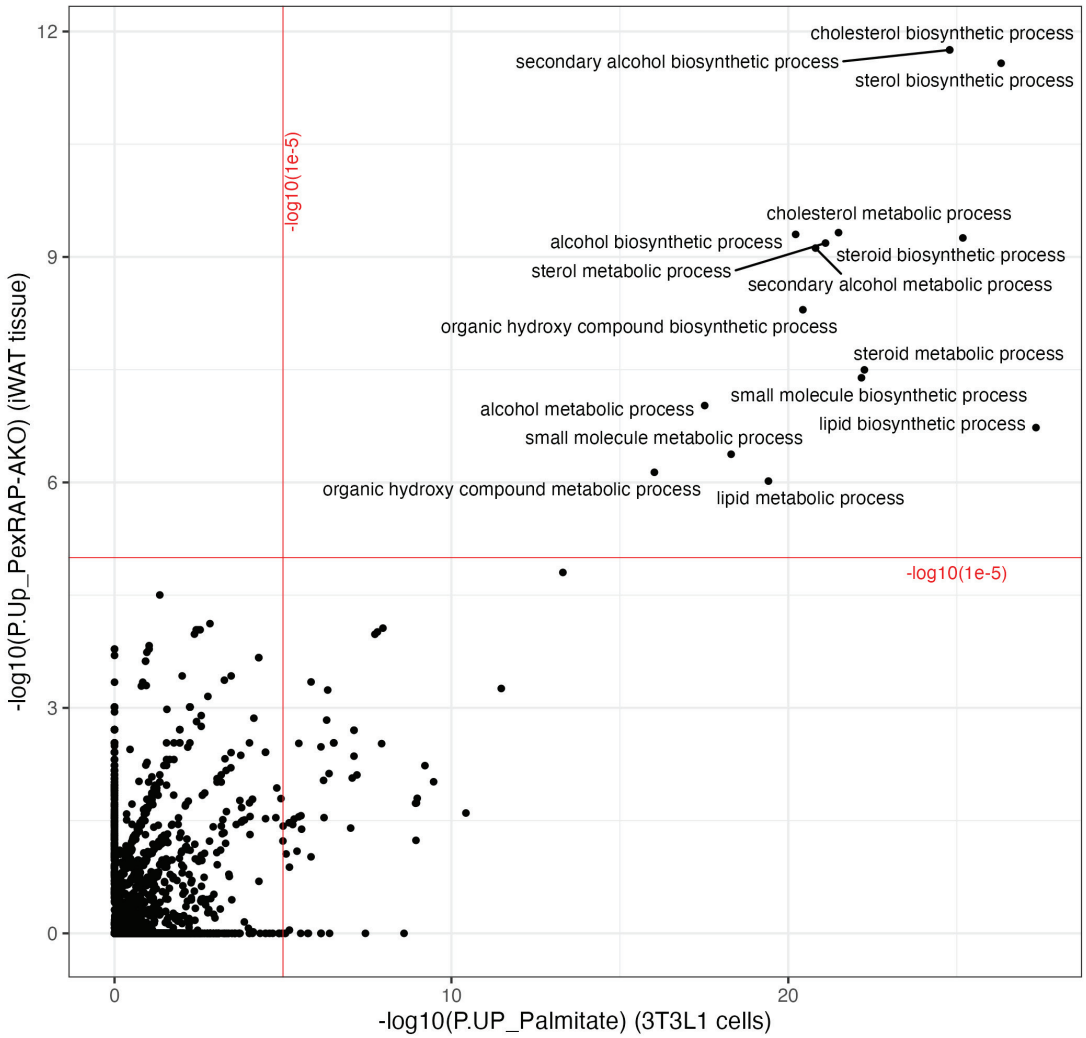

Supplementary Figure 5. Relationship between GO terms upregulated in iWAT of PexRAP-AKO mice and those upregulated in palmitate-treated 3T3-L1 adipocytes. Comparison plot of upregulated GO pathways in RNA-seq data from iWAT of male control and PexRAP-AKO mice (y-axis) versus in palmitate-treated 3T3-L1 adipocytes (x-axis) (GSE129442) (n = 3/condition for 3T3-L1 cells, 5/condition for control vs. PexRAP mice). Data are shown as mean ± SEM. Comparisons between groups were made with the hypergeometric test built into the R/Bioconductor limma::goana() pathway enrichment function.

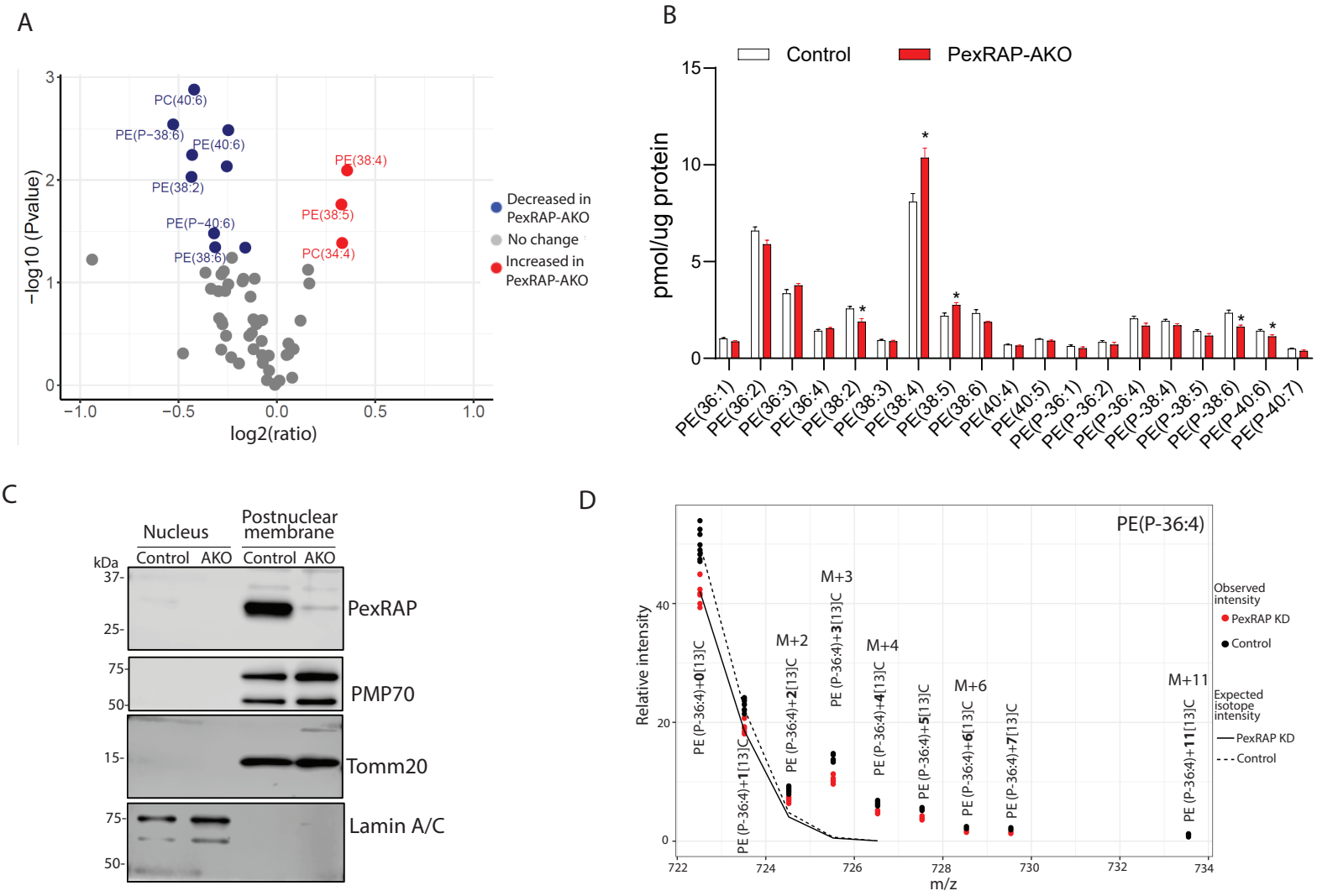

Supplementary Figure 6. Effect of PexRAP depletion on membrane phospholipids. Targeted ESI-MS analysis of PC and PE species from the postnuclear fraction of iWAT from HFD fed male control and PexRAP-AKO mice, expressed as **A**) logFC values (PexRAP-AKO versus Control) and **B**) absolute concentrations. **C**) Western blot analysis of nuclear and postnuclear membrane fractions of iWAT from HFD fed male control and PexRAP-AKO mice. **D**) All detected isotopes of PE(P-36:4) in control cells versus PexRAP-KD cells from a ESI-MS-based [13]Carbon-flux analysis of 3T3-L1 cells differentiated to white adipocytes, treated with scrambled (SC) or PexRAP shRNA, and then maintained in U[13]C-glucose containing media for 5 days.